The Journal of Physical Chemistry Letters

Letter

Cite This: J. Phys. Chem. Lett. 2019, 10, 1264−1271

pubs.acs.org/JPCL

Directed Gas-Phase Formation of the Germaniumsilylene Butterfly Molecule (Ge(μ-H_2)Si)

Aaron M. Thomas, Beni B. Dangi,[†] Tao Yang,[‡] György Tarczay,[§] and Ralf I. Kaiser*

Department of Chemistry, University of Hawai'i at Manoa, Honolulu, Hawaii 96822, United States

Bing-Jian Sun, Si-Ying Chen, and Agnes H. H. Chang*

Department of Chemistry, National Dong Hwa University, Shoufeng, Hualien 974, Taiwan

Thanh L. Nguyen and John F. Stanton*

Quantum Theory Project, Department of Chemistry and Physics, University of Florida, Gainesville, Florida 32611, United States

Alexander M. Mebel*

Florida International University, Miami, Florida 33199, United States

Samara University, Samara 443086, Russia

Supporting Information

ABSTRACT: The hitherto elusive dibridged germaniumsilylene molecule (Ge(μ-H_2)Si) has been formed for the first time via the bimolecular gas-phase reaction of ground-state germanium atoms (Ge) with silane (SiH_4) under single-collision conditions. Merged with state-of-the-art electronic structure calculations, the reaction was found to proceed through initial formation of a van der Waals complex in the entrance channel, insertion of the germanium into a silicon−hydrogen bond, intersystem crossing from the triplet to the singlet surface, hydrogen migrations, and eventually elimination of molecular hydrogen via a tight exit transition state, leading to the germaniumsilylene "butterfly". This investigation provides an extraordinary peek at the largely unknown silicon−germanium chemistry on the molecular level and sheds light on the essential nonadiabatic reaction dynamics of germanium and silicon, which are quite distinct from those of the isovalent carbon system, thus offering crucial insights that reveal exotic chemistry and intriguing chemical bonding in the germanium−silicon system on the most fundamental, microscopic level.

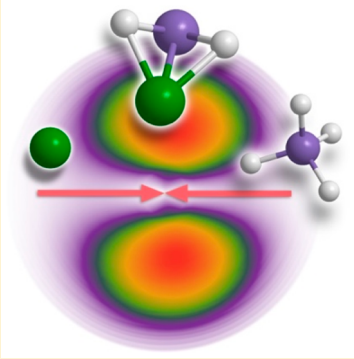

For one century, Langmuir's concept of isoelectronicity has been influential in expanding novel synthetic chemistry, in rationalizing the reactivity of isoelectronic systems, in developing modern concepts of chemical bonding, and in understanding basic concepts of molecular structure.[1] For the last decades, particular attention has been devoted to comparing the germanium and silicon chemistries with the analogous carbon chemistry.[2−5] Residing in main group XIV, carbon, silicon, and germanium each have four valence electrons and hence are isovalent.[6] Yet, their chemical bonding can be quite distinct, as demonstrated by the linear tricarbon molecule [C_3; (**1**)][7] strongly differing from the cyclic silicon dicarbide molecule [SiC_2; (**2**)][8] and the bent disilicon carbide [Si_2C; (**3**)][9] and trisilicon [Si_3; (**4**)][10] molecules (Figure 1). The diverse chemical bonding of carbon versus silicon and germanium is best reflected in a comparison of the homo- (E_2H_2) and heteronuclear ($EE'H_2$) dihydrides (Figure 2). Whereas the linear acetylene molecule (H−C≡C−H) (**5**)

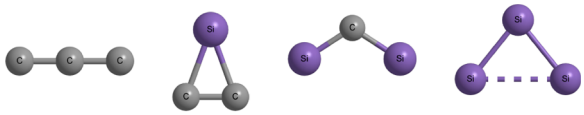

C_3	SiC_2	CSi_2	Si_3
$D_{\infty h}$	C_{2v}	C_{2v}	C_{2v}
(1)	(2)	(3)	(4)

Figure 1. Minimum-energy geometries and point groups of isovalent tricarbon (1), silicon dicarbide (2), disilicon carbide (3), and trisilicon (4); carbon and silicon atoms are color-coded in gray and purple, respectively.

Received: January 31, 2019
Accepted: February 28, 2019
Published: February 28, 2019

DOI: 10.1021/acs.jpclett.9b00284
J. Phys. Chem. Lett. 2019, 10, 1264−1271

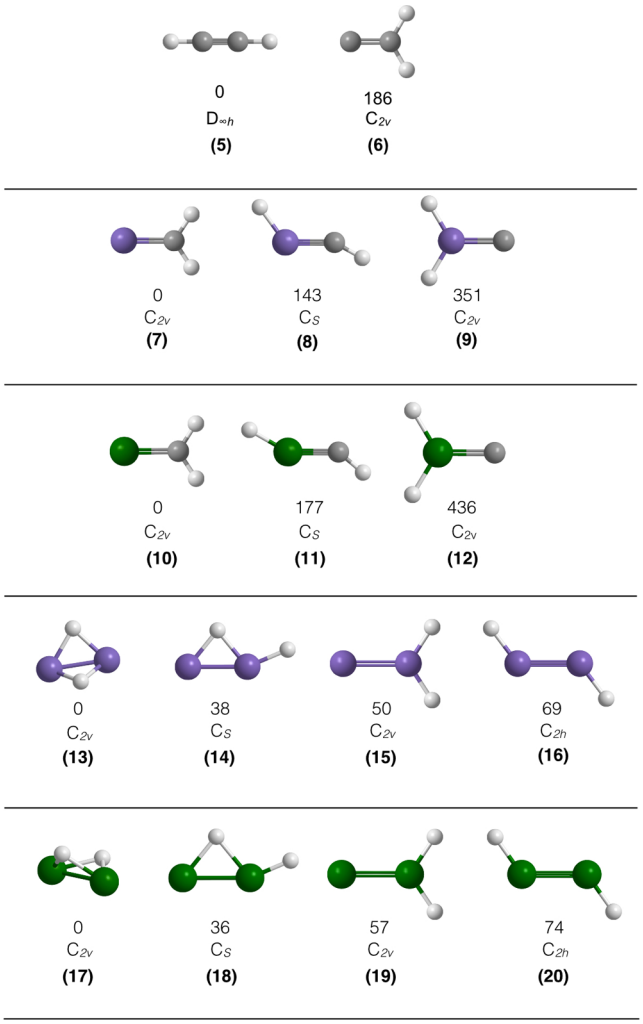

Figure 2. Structures, point groups, and relative energies (kJ mol^{-1}) of homo- and heteronuclear dihydrides of the main group XIV elements carbon (gray), silicon (purple), and germanium (green).

exemplifies the thermodynamically most stable isomer, with vinylidene carbene ($H_2C{=}C$) (**6**) less stable by 186 kJ mol^{-1},[11] the sequence of stability is reversed for the $SiCH_2$ and $GeCH_2$ isomers. Here, the silavinylidene ($H_2C{=}Si$) (**7**) and germavinylidene ($H_2C{=}Ge$) (**10**) molecules represent the global minima and are thermodynamically favored by 145 and 177 kJ mol^{-1} compared to the trans bent isomers silaacetylene ($HC{=}SiH$) (**8**) and germaacetylene ($HC{=}GeH$) (**11**).[12,13] This departure can be understood from the reduced overlap of the valence s and p orbitals of the silicon and germanium atoms as compared to carbon, which hinders their ability to form the sp orbital hybrids responsible for the linear geometry of acetylene.[14] The exotic chemical bonding and unusual molecular structures of silicon and germanium are demonstrated by spectroscopic detection of the nonclassical, hydrogen-bridged Si(μ-H_2)Si (**13**)[15]−HSi(μ-H)Si (**14**)[16] and Ge(μ-H_2)Ge (**17**)−HGe(μ-H)Ge (**18**) isomer pairs,[17] whose carbon−analogue structures do not exist as equilibrium structures. The hydrogen-bridged geometries are energetically favorable compared to their carbene [$H_2Si{=}Si$ (**15**), $H_2Ge{=}Ge$ (**19**)], and *trans*-acetylenic-type isomers [HSiSiH (**16**), HGeGeH (**20**)] (Figure 2).[12,18,19]

However, although substantial research has been conducted in understanding of the chemical bonding and structures of the homonuclear [C_2H_2, Si_2H_2, Ge_2H_2] and heteronuclear systems [$SiCH_2$, $GeCH_2$], a detailed experimental characterization of the formation of free heteronuclear $GeSiH_2$ molecules has remained elusive, with only substituted forms of the silagermenylidene ($Ge{=}SiH_2$) isomer being observed in the laboratory thus far.[20,21] Electronic structure calculations predict the existence of six structural isomers in their singlet electronic ground states, with the exotic Si(μ-H_2)Ge butterfly molecule being the thermodynamically most stable structure.[12] This reflects the preferential stability of hydrogen-bridged dinuclear molecules in the absence of carbon, which in contrast favors acetylenic or carbene-type structures. Therefore, replacement of both carbon atoms in acetylene by silicon and germanium is expected to lead to novel molecules, whose isovalent carbon counterparts do not exist, thus classifying the $GeSiH_2$ system as a prototype target to provide fundamental perspectives on chemical reactivity of silicon- and germanium-bearing species along with their chemical bonding.

Here, we report on the very first observation of the hitherto elusive germaniumsilylene butterfly molecule (Ge(μ-H_2)Si) under single-collision conditions in the gas phase by reacting ground-state germanium atoms (Ge(^3P_j)) with silane (SiH_4; X^1A_1), exploiting the crossed molecular beam method and combining the experimental data with electronic structure calculations. This system represents a benchmark to explore the consequence of a single-collision event with the simplest germanium-bearing open-shell species (atomic germanium) with the prototype closed-shell silicon-carrying molecule (silane). The chemical reaction proceeds via a van der Waals complex in the entrance channel followed by isomerization and insertion of germanium into the silicon−hydrogen bond, nonadiabatic dynamics through intersystem crossing (ISC) from the triplet to the singlet surface, hydrogen migrations, and eventually unimolecular decomposition by molecular hydrogen elimination via a tight exit transition state, leading to the dibridged Ge(μ-H_2)Si isomer. These findings act as a benchmark to shed light on an unusual germanium−silicon chemistry and strongly diverge from those of isovalent carbon-based systems.

The reactive scattering experiments were performed using a crossed molecular beam apparatus (Methods). Accounting for the natural isotope abundances of silicon [^{30}Si (3.1%), ^{29}Si (4.67%), ^{28}Si (92.23%)] and of germanium [^{70}Ge (20.4%), ^{72}Ge (27.3%), ^{73}Ge (7.7%), ^{74}Ge (36.7%), and ^{76}Ge (7.8%)], reactive scattering signal was explored from mass-to-charge (m/z) of m/z = 110 ($^{76}Ge^{30}SiH_4^+$) to m/z = 98 ($^{70}Ge^{28}Si^+$), with the signal at m/z = 104 ($^{74}Ge\ ^{28}SiH_2^+$) depicting the best signal-to-noise. It is important to note that after scaling the TOF spectra recorded at different mass-to-charge ratios reveal identical patterns suggesting the existence of a single channel; no signal of any $GeSiH_4$ adduct could be observed. On the basis of these considerations, the angular-resolved TOF spectra were taken at m/z = 104 ($^{74}Ge\ ^{28}SiH_2^+$) with the laboratory angular distribution spread over 28° within the scattering plane, as defined by atomic germanium and silane reactant beams (Figures 3 and 4). The nearly forward−backward symmetry with respect to the center-of-mass (CM) of 23.2 ± 0.2° suggests that the reaction of ground-state germanium atoms with silane involves indirect reaction dynamics through the formation of $^{74}Ge^{28}SiH_4$ complex(es). The unimolecular decomposition of the intermediate(s) forms a molecule with the formula $^{74}Ge^{28}SiH_2$ (hereafter $GeSiH_2$) via molecular hydrogen loss. Note that ions at higher (109−105) and lower

DOI: 10.1021/acs.jpclett.9b00284
J. Phys. Chem. Lett. 2019, 10, 1264−1271

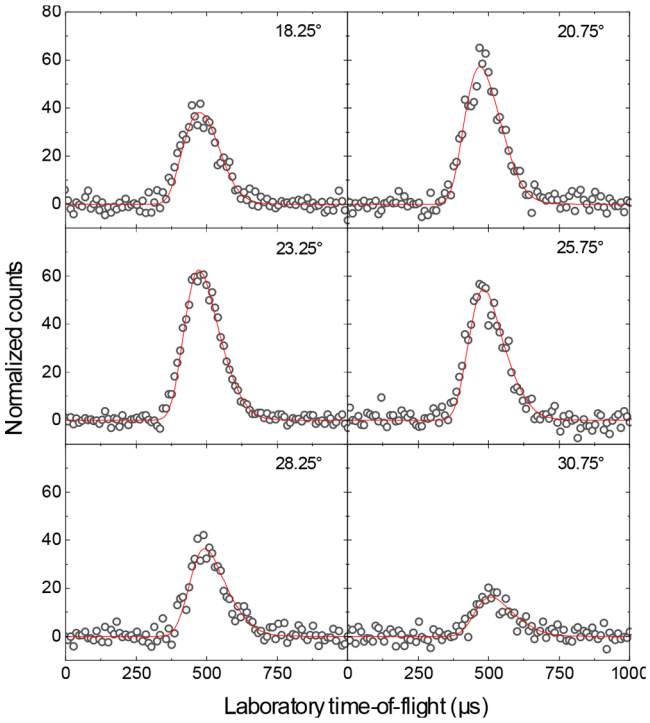

Figure 3. Time-of-flight spectra recorded at distinct laboratory angles at m/z = 104 ($^{74}GeSiH_2^+$) for the reaction of ground-state germanium ($^{74}Ge(^3P_j)$) atoms with silane (SiH_4; X^1A_1). The open circles indicate the experimentally measured data and red lines the best fits.

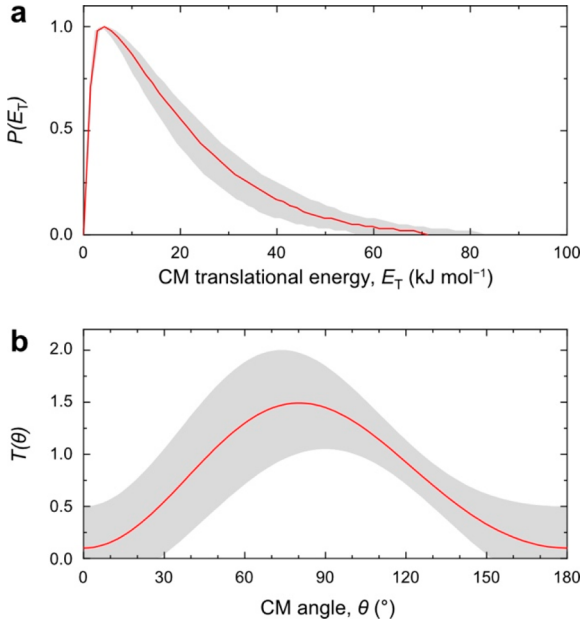

Figure 5. CM translational energy (a) and angular (b) flux distributions of $^{74}GeSiH_2$ produced from the reactive scattering of germanium ($^{74}Ge(^3P_j)$) with silane (SiH_4; X^1A_1). Shaded areas indicate the acceptable upper and lower error limits of the fits accounting for the uncertainties of the laboratory angular distribution and time-of-flight spectra, with the red solid lines defining the best-fit functions.

(103−98) mass-to-charge ratios are linked to isotopologues and/or isotopomers of ^{74}Ge $^{28}SiH_2^+$ and their fragment ions generated upon electron impact ionization of the neutral ^{74}Ge $^{28}SiH_2$ product in the electron impact ionizer.

Our objective extends beyond establishing the chemical formula of the reaction product to rationalizing its structure and the underlying reaction mechanism governing its formation. This requires transformation of the laboratory experimental data obtained at m/z = 104 ($GeSiH_2^+$) into the CM reference frame. Figure 5a shows the resulting best fit CM translational energy $P(E_T)$ and angular flux $T(\theta)$ distributions along with the error limits. Importantly, the laboratory data were fit with a single product channel of a mass combination of 104 amu ($GeSiH_2$) and 2 amu (H_2); it is critical to stress that the formation of any $GeSiH_3$ isomer via atomic hydrogen loss is highly endoergic by at least 120 kJ mol^{-1}[22] and hence is closed under our experimental conditions. It is critical to stress that fits of the experimental data could only be achieved by

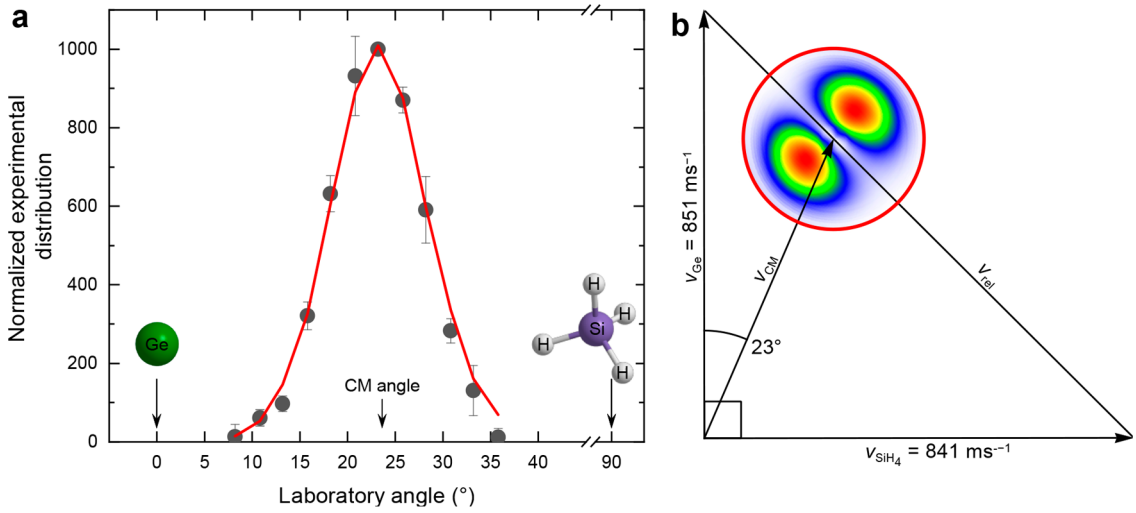

Figure 4. Laboratory angular distribution and Newton diagram with associated $GeSiH_2$ flux contour map. (a) Laboratory angular distribution of ion signal obtained at mass-to-charge ratio 104 ($^{74}GeSiH_2^+$) for the reaction of ground-state germanium ($^{74}Ge(^3P_j)$) atoms with silane (SiH_4; X^1A_1). The incident germanium and silane beams are indicated at 0 and 90°, respectively. The black dots indicate the experimental data with $\pm 1\sigma$ uncertainty, and the red line indicates the best fit. (b) Corresponding Newton diagram of the germanium−silane system; the red circle holds a radius equivalent to the maximum CM velocity of the thermodynamically most stable $^{74}GeSiH_2$ isomer with the flux contour map inset.

DOI: 10.1021/acs.jpclett.9b00284
J. Phys. Chem. Lett. 2019, 10, 1264−1271

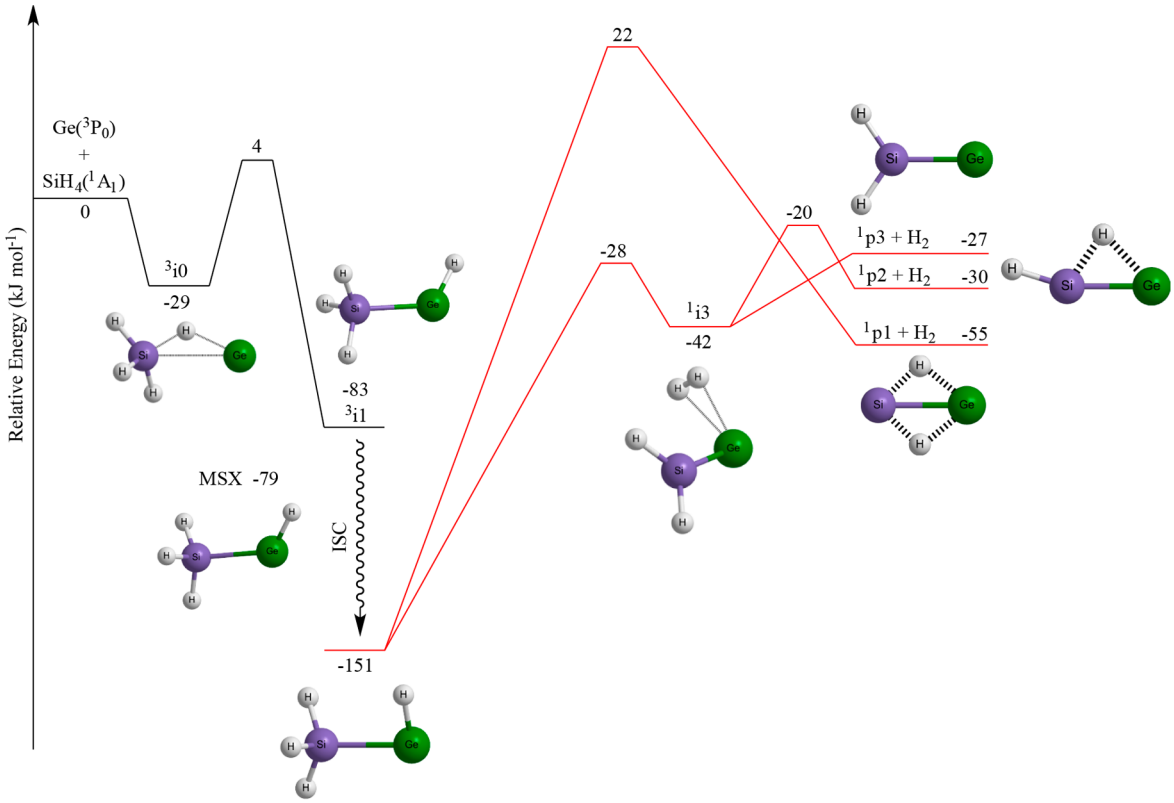

Figure 6. Section of the relevant PES of the reaction of ground-state atomic germanium (Ge ($^3P_0$)) with silane (SiH_4; X^1A_1). The minimal-energy crossing point (MSX) is shown for ISC from the triplet surface (black) to the singlet surface (red).

incorporating a reaction threshold of 14−16 kJ mol^{-1} into the fitting routine, i.e., a threshold energy of the colliding germanium atom and silane molecules must have to form at least one of the $GeSiH_2$ species. Inspecting the CM translational energy flux distribution, $P(E_T)$, the maximum translational energy (E_{max} = 71 ± 14 kJ mol^{-1}) of the products helps to identify the nature of the $GeSiH_2$ isomer. For molecules born without rovibrational excitation, E_{max} characterizes the sum of the reaction exothermicity and the collision energy. Therefore, subtraction of the collision energy (16 kJ mol^{-1}) suggests that the formation of $GeSiH_2$ plus molecular hydrogen is exothermic by 55 ± 14 kJ mol^{-1}. The $GeSiH_2$ isomer formed can be assigned by comparing the experimentally determined reaction exothermicity with the energetics obtained from electronic structure computations for distinct $GeSiH_2$ isomers (Figure S1). The experimental reaction energy agrees exceptionally well with the computed energy of −55 ± 4 kJ mol^{-1} to form the thermodynamically most stable Ge(μ-H_2)Si (^{1}**p1**) molecule in its ^{1}A′ electronic ground state. The cis-monobridged Ge(μ-H)SiH (^{1}**p2**) and Ge═SiH_2 (^{1}**p3**) isomers are less stable by 25 and 28 kJ mol^{-1}; this would result in reaction energies of −30 ± 4 and −27 ± 4 kJ mol^{-1}, respectively. Therefore, ^{1}**p2** and ^{1}**p3** along with higher-energy isomers ^{1}**p3**−^{1}**p6** might be formed as well and might be masked in the low-energy part of the CM translational energy distribution. We note that these energies are given for germanium atoms formed in their $^3P_0$ electronic ground state. The j = 1 and 2 states are higher in energy by 6.7 and 16.9 kJ mol^{-1}. For Ge(μ-H)SiH (^{1}**p2**) and Ge═SiH_2 (^{1}**p3**), this would yield reaction energies of 37 ± 14 kJ mol^{-1} (j = 1) and 47 ± 14 kJ mol^{-1} (j = 2) for ^{1}**p2** and 34 ± 14 kJ mol^{-1} (j = 1) and 44 ± 14 kJ mol^{-1} (j = 2) for ^{1}**p2**. Hence, within the error limits, we believe that at least the thermodynamically most stable Ge(μ-H_2)Si (^{1}**p1**) isomer is formed from reaction of germanium in its $^3P_0$ ground state with higher-energy isomers possibly masked in the low-energy part of the CM translational energy distribution. Among potential triplet products, even the energetically most favorable isomer ^{3}**p3** (+14 ± 4 kJ mol^{-1}) does not correlate with the experimentally derived reaction energy of −55 ± 14 kJ mol^{-1}. Therefore, we conclude that because the reaction of ground-state atomic germanium with silane starts on the triplet surface but the energetically feasible product(s) hold singlet ground states, at least one channel of the reaction involves ISC and hence nonadiabatic reaction dynamics. Finally, the CM angular distribution, $T(\theta)$, has intensity over the complete angular range from 0 to 180° (Figure 5b). This finding implies indirect scattering dynamics through the formation of $GeSiH_4$ complex(es) holding lifetimes longer than their rotational periods.[23] Note that best fits were achieved with a distribution maximum at 80°, implying geometrical constraints of the exit transition state(s) with the hydrogen molecule emitted perpendicularly to the plane of the decomposing complex almost parallel to the total angular momentum vector. In conclusion, at least the thermodynamically most stable germaniumsilylene molecule (Ge(μ-H_2)Si) (^{1}**p1**) is formed from reaction of germanium in its $^3P_0$ ground state with silane involving nonadiabatic reaction dynamics and ISC from the triplet to the singlet surface.

We are now combining the aforementioned discussion with the computational results to unravel the underlying reaction mechanism(s) (Figures 6 and S1−S6). Because the energetically accessible product isomers (^{1}**p1**−^{1}**p6**) plus molecular hydrogen have singlet ground states but the bimolecular

DOI: 10.1021/acs.jpclett.9b00284
J. Phys. Chem. Lett. 2019, 10, 1264−1271

collision is initiated on the triplet surface, potential molecular hydrogen loss channels are explored on both triplet and singlet $GeSiH_4$ potential energy surfaces (PESs) together with ISC. The formation of any $GeSiH_3$ isomer via atomic hydrogen loss is highly endoergic by at least 120 kJ mol^{-1},[22] and hence closed at the experimental collision energy of 16 kJ mol^{-1}. The complete PES is very complex (Figure S2), containing 10 intermediates and 18 transition states. The complexity of this surface requires a simplification. Considering the experimental collision energy of 16 kJ mol^{-1}, all transition states and products above this energy—accounting for the accuracy of the calculations—cannot be overcome in our crossed beam study. The removal of these transition states and energetically inaccessible products results in a simplified PES that contains only four intermediates, four transition states, and three possible product channels (Figure 6).

Our calculations expose that the reaction is initiated on the triplet surface via defacto insertion of the germanium atom into the silicon−hydrogen bond of silane. Once the germanium atom approaches the silane molecule, the PES is attractive and results in a van der Waals complex ^{3}**i0** that is stabilized by 29 kJ mol^{-1} with respect to the separated reactants. This complex can rearrange through insertion of the germanium atom into the silicon−hydrogen bond of silane involving a barrier of 33 kJ mol^{-1}. This leads to the covalently bound reaction intermediate ^{3}**i1** silylgermylene (H_3SiGeH). The transition state connecting the van der Waals complex ^{3}**i0** and intermediate ^{3}**i1** is only slightly higher in energy by 4 kJ mol^{-1} than the separated reactants and can be passed easily considering the collision energy of 16 kJ mol^{-1}. We also located a transition state connecting intermediate ^{3}**i1** to the thermodynamically most stable triplet product (^{3}**p3**) that lies 86 kJ mol^{-1} *above* the energy of the separated reactants. Therefore, at a collision energy of 16 kJ mol^{-1}, the pathway even to the energetically most stable triplet isomer is closed (Figure S2), confirming our earlier conclusion that under our experimental conditions, triplet $GeSiH_2$ isomers are not formed in the bimolecular reaction of ground-state germanium atoms with silane.

The computations predict that ^{3}**i1** undergoes ISC to intermediate ^{1}**i1**, which resides in a deep potential energy well of 151 kJ mol^{-1} with respect to the separated reactants. The seam of crossing (MSX) between the triplet structure ^{3}**i1** and ^{1}**i1** located a crossing point between the lowest triplet and singlet electronic states of intermediate ^{1}**i1** close to ^{3}**i1**. The seam of crossing is 79 kJ mol^{-1} in energy below the separated reactants, slightly above ^{3}[**i1**]. What is the fate of ^{1}**i1**? Our calculations reveal that H_3SiGeH can undergo unimolecular decomposition to Ge(μ-H_2)Si (^{1}**p1**) via a tight transition state located 22 ± 4 kJ mol^{-1} above the separated reactants (Figure S3). Recall that the experimental data could *only* be replicated by incorporating a reaction threshold of 14−20 kJ mol^{-1} into the fitting routine, which agrees nicely with the computed barrier. Regarding the exit transition state connecting H_3SiGeH (^{1}**i1**) to Ge(μ-H_2)Si (^{1}**p1**), our electronic structure calculations suggest that molecular hydrogen departs the dissociating complex at angles with respect to the principal axes *A*, *B*, and *C* of 81.5, 11.1, and 82.9°, respectively (Figure S4). Close inspection of the principal moments of inertia reveal that the $^{74}Ge^{28}SiH_4$ decomposing structure is a near-prolate complex with I_a (2.00 × 10^{-46} kg m^2) < I_b (2.17 × 10^{-45} kg m^2) ≈ I_c (2.28 × 10^{-45} kg m^2), and in the prolate limit, molecular hydrogen emission perpendicular to the symmetric axis (81.5°) results in sideways scattering.[24] The geometry of the dissociating complex to form ^{1}**p1** therefore agrees well with the $T(\theta)$ distribution maximum at 80° (Figure 5b) derived from experiment. Considering the inherent barriers to isomerization of the reaction intermediates, H_3SiGeH (^{1}**i1**) is also expected to eliminate molecular hydrogen via a four-center elimination, leading to the van der Waals complex ^{1}**i3**. The decay of this complex yields either silagermenylidene (Ge═SiH_2; ^{1}**p3**) via barrierless dissociation (Figure S5) or Ge(μ-H)SiH (^{1}**p2**) via a relatively loose transition state (Figure S6). It should be noted that intermediates ^{1}**i2** and ^{1}**i4**−^{1}**i7** are also energetically accessible at our collision energy via isomerization of ^{1}**i1** (Figure S2). However, unimolecular decomposition of these structures via molecular hydrogen loss leads to $GeSiH_2$ isomers whose energetics do not account for the experimentally derived reaction energy of −55 ± 14 kJ mol^{-1}.

In summary, the experimental data and computations propose that at least the thermodynamically most stable Ge(μ-H_2)Si (^{1}**p1**) molecule is formed via nonadiabatic reaction dynamics in the reaction of ground-state germanium atoms plus silane. Considering the inherent barriers to isomerization of the reaction intermediates, the Ge(μ-H)Si (^{1}**p2**) and Ge═SiH_2 (^{1}**p3**) isomers likely contribute the reactive scattering signal as well, but a quantification represents a tricky problem and is beyond the scope of the present study as this investigation would require the consideration of spin−orbit coupling and the exact branching ratios of the $^3P_0$, $^3P_1$, and $^3P_2$ states for the atomic germanium reactant. Despite these open questions, single-collision conditions provide an ideal tool to form novel molecules such as dibridged germaniumsilylene (Ge(μ-H_2)Si) (^{1}**p1**).

Our combined experimental and theoretical investigation of the bimolecular reaction of ground-state germanium atoms with silane exposes overall exothermic channels to the previously elusive germaniumsilylene molecule (Ge(μ-H_2)Si) (^{1}**p1**) under single-collision conditions in the gas phase. This reaction begins on the triplet surface via formation of a van der Waals complex followed by isomerization through insertion of the germanium atom into a silicon−hydrogen bond of the silane molecule, yielding the silylgermylene (H_3SiGeH) intermediate. This intermediate is predicted to undergo ISC to singlet H_3SiGeH, which undergoes unimolecular decomposition via molecular hydrogen loss to Ge(μ-H_2)Si (^{1}**p1**) involving a tight exit transition state in an overall exoergic reaction. It is critical to recall that a fit of the laboratory data could *only* be obtained through the incorporation of a reaction threshold of 14−20 kJ mol^{-1} into the fitting routine. This energy correlates closely with the computed energy of the transition state connecting ^{1}**i1** and ^{1}**p1** plus molecular hydrogen of 22 ± 4 kJ mol^{-1}; however, our experimental data and, in particular, the relevant PES (Figure 6) do not exclude the potential formation of ^{1}**p2** and/or ^{1}**p3** as well. Carrying a 0.61 D dipole moment (Table S8), the C_s symmetric Ge(μ-H_2)Si (^{1}**p1**) is stabilized by one σ-bond and two donor−acceptor bonds that form two three-center/two-electron hydrogen bridges; it has no π-bonds.[25] The hydrogen atoms and heavy nuclei occupy separate planes, and the 104.5° dihedral between them is geometrically reminiscent of a perched butterfly. It is worth noting that silicon and germanium are metalloids and that the geometry and bonding of Ge(μ-H_2)Si are strikingly consistent with those of the isoelectronic diborane[4] (HB(μ-H_2)BH),[26] which is also

DOI: 10.1021/acs.jpclett.9b00284
J. Phys. Chem. Lett. 2019, 10, 1264−1271

stabilized by one σ-bond and two three-center/two-electron hydrogen bridges and adopts a butterfly configuration.

Despite sharing the same period, the differences in the equilibrium geometries of the dicarbon hydrides and the silicon−germanium hydrides are tremendous, as documented in numerous detailed computational reports over the last decades. More recently, theory and experiment have come together in an effort to connect exotic molecules like Ge(μ-H_2)Si to bimolecular gas-phase reactants, as was done in this study, to understand exactly how these molecules form by evaluating the reactivity of group XIV atoms with their tetrahydrides. In the simplest case, the reaction of the ground-state carbon ($C(^3P)$) atom with methane (CH_4) is initially attractive due to a weakly bound van der Waals complex, but the pathways leading to triplet C_2H_2 isomers are inhibited by a 51 kJ mol^{-1} (0 K) barrier[27] and hence closed under identical experimental conditions in crossed molecular beam experiments. Compared to the carbon−methane system, replacing $C(^3P)$ with a silicon ($Si(^3P)$) atom results in low-energy pathways to triplet *and* singlet $SiCH_2$ isomers whose features lie below the energy of the separated $Si(^3P)$ and CH_4 reactants, enabling the reaction to proceed spontaneously,[28] and when both carbon atoms are replaced with silicon atoms, both the spontaneity and exotic structures familiar to the present study are open to the reactants.[18] $Si(^3P)$ insertion at silane (SiH_4) is mitigated by a low-lying van der Waals interaction, and the resulting Si_2H_4 complex eliminates molecular hydrogen to form singlet disilavinylidene ($H_2SiSi(^1A_1)$),[18] which, as illustrated in Figure 2, is *not* the thermodynamically favored Si_2H_2 isomer. Importantly, as uncovered in the present study, substituting $Si(^3P)$ with $Ge(^3P)$ further alters the reaction dynamics such that the minimum-energy isomer, here the dibridged germaniumsilylene (^{1}**p1**) molecule, is selected as the nascent reaction product following insertion of $Ge(^3P)$ into SiH_4.

The reaction dynamics of the germanium−silane system are clearly distinct as compared to those of isovalent systems comprising a carbon or silicon atom that reacts with methane or silane. Further, the incredibly varied differences uncovered by the systematic substitution of carbon atoms in the $C(^3P)$ + CH_4 reaction with silicon and/or germanium reveal that the data accrued in deceptively analogous reaction systems differ so strongly that insight from one reaction system is not readily leveraged toward interpreting another. That chemical intuition is not sufficient for predicting the reactivity of heavy group XIV atoms in what are seemingly similar and simple (six atoms) isovalent reaction systems affects how we think about the reaction dynamics of isovalent systems and the chemical bonding of germanium- and silicon-bearing molecules. The germanium−silane system therefore serves as a critical benchmark toward an intimate understanding of the formation of hitherto elusive silicon- and germanium-bearing molecules, thus influencing the conception of chemical structure and exotic chemical bonding in the future.

■ METHODS

Experimental Methods. The reaction between ground-state atomic germanium ($Ge(^3P_j)$) and silane (SiH_4; X^1A_1) was carried out in the gas phase at the molecular level under single-collision conditions exploiting a crossed molecular beam machine[29] coupled with a laser ablation source.[30] Briefly, a pulsed supersonic beam of ground-state germanium atoms was prepared in situ by laser ablation[30] of an optical-grade germanium rod (Alfa Aesar) at 266 nm (30 Hz; 3.3 mJ pulse^{-1}) and subsequently seeding the ablated germanium atoms in neon (Ne, 99.9999%, Matheson) gas, which was released by a pulsed valve operated at 60 Hz and a backing pressure of 3040 Torr. No higher germanium clusters were observed under these experimental conditions. The germanium atom beam was collimated by a skimmer, velocity-selected (peak velocity v_p = 851 ± 2 m s^{-1}; speed ratio S = 7.8 ± 0.1) and then perpendicularly crossed with a pulsed supersonic beam of pure silane (SiH_4, 99.999%, Voltaix, 550 Torr) with a peak velocity of 841 ± 10 ms^{-1} and a speed ratio of 10.2 ± 0.3 in the scattering chamber at a collision energy of 16.0 ± 0.2 kJ mol^{-1}. The reaction products were monitored by a rotatable quadrupole mass spectrometer after electron impact ionization of the neutral products at 80 eV in an ultrahigh-vacuum chamber. The velocity distributions of the products were recorded through the angular-resolved time-of-flight (TOF) technique by recording the arrival time of the ions at well-defined mass-to-charge ratios (m/z) of the ionized products at different scattering angles. The TOF spectra at each angle were then integrated to obtain the laboratory angular distribution. To allow a "laser-on" minus "laser-off" background subtraction, both valves were triggered at 60 Hz, but the laser was operated at half of the frequency at 30 Hz. To extract information on the chemical dynamics and hence the reaction mechanism from the experimental data, a forward convolution fitting technique was applied. This approach simulates the laboratory data (TOF spectra, laboratory angular distribution) of the reactively scattered products and yields two "best-fit" functions: the CM translational energy flux distribution $P(E_T)$ and the angular flux distribution $T(\theta)$.[31,32] Finally, we note that in its ^3P electronic ground state, three j levels (0, 1, 2) can be populated, with j = 1 and 2 lying 6.7 and 16.9 kJ mol^{-1} higher in energy than j = 0.[33] Therefore, we characterized the j-level distribution of the germanium atoms in their ground electronic states (^3P) employing laser-induced fluorescence (LIF). These data suggest the presence of atomic germanium in the $^3P_0$, $^3P_1$, and $^3P_2$ states.

Computational Methods. The reaction of ground-state atomic germanium ($Ge(^3P)$) with silane (SiH_4; X^1A_1) is also explored theoretically. The geometries of possible triplet and singlet $GeSiH_2$ and $GeSiH_4$ isomers are optimized via coupled cluster[34−37] CCSD/cc-pVTZ calculations. The complete basis set limits,[38] CCSD(T)/CBS energies, are obtained by extrapolating the CCSD(T)/cc-pVDZ, CCSD(T)/cc-pVTZ, and CCSD(T)/cc-pVQZ energies, with CCSD/cc-pVTZ zero-point energy corrections. The accuracy of these CCSD(T)/CBS energies are expected to be within 4 kJ mol^{-1}.[39] The minimum-energy crossing point between ^{3}**i1** and ^{1}**i1** was located with the CPMCSCF[40]/TZVPP method with energy refined via CCSD(T)/CBS. GAUSSIAN09 programs[41] were used in density functional and coupled cluster calculations, and MOLPRO[40] was exploited for the surface-crossing computations. To verify the overall energetics of the reactions and the relative stabilities of the triplet and singlet $GeSiH_2$ isomers, a modified HEAT-345(Q) approach (designated hereafter as mHEAT-345(Q)), which was previously applied to medium-sized molecules, was exploited.[42,43]

$$E_{\mathrm{mHEAT}} = E^{\infty}_{\mathrm{SCF}} + \Delta E^{\infty}_{\mathrm{CCSD(T)}} + \Delta E_{\mathrm{T-(T)}} + \Delta E_{\mathrm{(Q)-T}} + \Delta E_{\mathrm{ZPE}} + \Delta E_{\mathrm{DBOC}} + \Delta E_{\mathrm{Scalar}} \quad (1)$$

The composite method mHEAT-345(Q) is defined as follows: (i) It uses a molecular structure, which is fully

DOI: 10.1021/acs.jpclett.9b00284
J. Phys. Chem. Lett. 2019, 10, 1264−1271

optimized with the frozen-core (FC) CCSD(T)/ANO1 level of theory; (ii) Hartree–Fock energy is extrapolated to a complete basis set using Dunning's basis sets,[38,44] specifically cc-pVTZ, cc-pVQZ, and cc-pV5Z; (iii) an electron-correlation energy with the CCSD(T) method is obtained by an extrapolation based on the cc-pVQZ and cc-pV5Z basis sets (in these calculations, all core electrons are frozen); (iv) high-level correction (HLC) is calculated as a sum of two contributions, i.e., a full triple correction and a quadruple excitation correction from perturbation theory; the former is calculated as a difference in energy between FC-CCSDT/cc-pVTZ and FC-CCSD(T)/cc-pVTZ, while the latter is obtained from the difference between FC-CCSDT(Q)/cc-pVDZ and FC-CCSDT/cc-pVDZ; (v) the anharmonic zero-point vibrational energy (ZPE) is calculated using FC-CCSD(T) and the atomic natural basis set[45−47] based on second-order vibration perturbation theory (VPT2).[48,49] Like the HEAT protocol, other small corrections such as scalar relativity effects and diagonal Born–Oppenheimer correction (DBOC) are also included. It is expected that mHEAT calculations give an accuracy of about 4 kJ mol^{-1} for relative energies. All calculations are done using the CFOUR quantum chemistry package.[50]

■ ASSOCIATED CONTENT

Supporting Information

The Supporting Information is available free of charge on the ACS Publications website at DOI: 10.1021/acs.jpclett.9b00284.

Details on the triplet and singlet $GeSiH_4$ potential energy surfaces including energies, vibrational frequencies, Cartesian coordinates, rotational constants, and dipole moments of intermediates, transition states, and reaction products (PDF)

■ AUTHOR INFORMATION

ORCID

Aaron M. Thomas: 0000-0001-8540-9523
Tao Yang: 0000-0003-4101-2385
György Tarczay: 0000-0002-2345-1774
Ralf I. Kaiser: 0000-0002-7233-7206
Thanh L. Nguyen: 0000-0002-7794-9439
John F. Stanton: 0000-0003-2345-9781
Alexander M. Mebel: 0000-0002-7233-3133

Present Addresses

†Department of Chemistry, Florida Agricultural and Mechanical University, Tallahassee, FL 32307, U.S.A.
‡State Key Laboratory of Precision Spectroscopy, East China Normal University, Shanghai 200062, China,
§Visiting Fulbright Professor; Permanent Address: Laboratory of Molecular Spectroscopy, Institute of Chemistry, Eötvös University, PO Box 32, H-1518 Budapest 112, Hungary

Author Contributions

A.M.T, B.B.D., T.Y., G.Y., and R.I.K. carried out the experimental measurements and data analysis. B.-J.S., S.-Y.C., A.H.H.C., T.L.N., J.F.S., and A.M.M. performed the theoretical calculations. All authors discussed the results and contributed to the manuscript.

Notes

The authors declare no competing financial interest.

■ ACKNOWLEDGMENTS

This work was supported by the U.S. National Science Foundation (NSF) for support under Award CHE-1360658 (A.M.T., B.B.D., T.Y., G.T., R.I.K.). Computer resources at the National Center for High-Performance Computer of Taiwan were utilized in the calculations (B.-J.S., S.-Y.C., A.H.H.C.). T.L.N. and J.F.S. were supported by the U.S. Department of Energy, Office of Basic Energy Sciences under Award Number DE-FG02-07ER15884. A.M.M.'s work during his visit to Samara University was supported by the Government of the Russian Federation under Grant No. 14.Y26.31.0020.

■ REFERENCES

(1) Langmuir, I. The Arrangement of Electrons in Atoms and Molecules. *J. Am. Chem. Soc.* **1919**, *41*, 868–934.
(2) Lischka, H.; Koehler, H. J. Ab Initio Investigation on the Lowest Singlet and Triplet State of Disilyne (Si_2H_2). *J. Am. Chem. Soc.* **1983**, *105*, 6646–6649.
(3) Binkley, J. S. Theoretical Study of the Relative Stabilities of C_2H_2 and Si_2H_2 Conformers. *J. Am. Chem. Soc.* **1984**, *106*, 603–609.
(4) Palágyi, Z.; Schaefer, H. F.; Kapuy, E. Ge_2H_2: A Germanium-Containing Molecule with a Low-Lying Monobridged Equilibrium Geometry. *J. Am. Chem. Soc.* **1993**, *115*, 6901–6903.
(5) Wang, Y.; Xie, Y.; Wei, P.; King, R. B.; Schaefer, H. F.; Schleyer, P. v. R.; Robinson, G. H. A Stable Silicon(0) Compound with a Si=Si Double Bond. *Science* **2008**, *321*, 1069.
(6) Babaev, E.; Hefferlin, R. The Concepts of Periodicity and Hyper-Periodicity: From Atoms to Molecules. In *Concepts in Chemistry: A Contemporary Challenge*, Rouvray, D., Ed.; Research Studies Press: London, 1996; pp 24–81.
(7) Mebel, A. M.; Kaiser, R. I. An Ab Initio Study on the Formation of Interstellar Tricarbon Isomers l-$C_3(X^1\Sigma_g^+)$ and c-$C_3(X^3A_2')$. *Chem. Phys. Lett.* **2002**, *360*, 139–143.
(8) Koput, J. Ab Initio Potential Energy Surface and Vibration-Rotation Energy Levels of Silicon Dicarbide, SiC_2. *J. Comput. Chem.* **2016**, *37*, 2395–2402.
(9) McCarthy, M. C.; Baraban, J. H.; Changala, P. B.; Stanton, J. F.; Martin-Drumel, M.-A.; Thorwirth, S.; Gottlieb, C. A.; Reilly, N. J. Discovery of a Missing Link: Detection and Structure of the Elusive Disilicon Carbide Cluster. *J. Phys. Chem. Lett.* **2015**, *6*, 2107–2111.
(10) McCarthy, M. C.; Thaddeus, P. Rotational Spectrum and Structure of Si_3. *Phys. Rev. Lett.* **2003**, *90*, 213003.
(11) DeVine, J. A.; Weichman, M. L.; Zhou, X.; Ma, J.; Jiang, B.; Guo, H.; Neumark, D. M. Non-Adiabatic Effects on Excited States of Vinylidene Observed with Slow Photoelectron Velocity-Map Imaging. *J. Am. Chem. Soc.* **2016**, *138*, 16417–16425.
(12) Boone, A. J.; Magers, D. H.; Leszczyński, J. Searches on the potential energy hypersurfaces of $GeCH_2$, $GeSiH_2$, and Ge_2H_2. *Int. J. Quantum Chem.* **1998**, *70*, 925–932.
(13) Lu, T.; Hao, Q.; Wilke, J. J.; Yamaguchi, Y.; Fang, D.-C.; Schaefer, H. F., Iii Silylidene ($SiCH_2$) and its Isomers: Anharmonic Rovibrational Analyses for Silylidene, Silaacetylene, and Silavinylidene. *J. Mol. Struct.* **2012**, *1009*, 103–110.
(14) Galbraith, J. M.; Schaefer, H. F. Hydrogen Bridging in Molecules Containing Atoms Beyond the First Row. *J. Mol. Struct.: THEOCHEM* **1998**, *424*, 7–20.
(15) Bogey, M.; Bolvin, H.; Demuynck, C.; Destombes, J. L. Nonclassical Double-Bridged Structure in Silicon-Containing Molecules: Experimental Evidence in Si_2H_2 from its Submillimeter-Wave Spectrum. *Phys. Rev. Lett.* **1991**, *66*, 413–416.
(16) Cordonnier, M.; Bogey, M.; Demuynck, C.; Destombes, J. L. Nonclassical Structures in Silicon-Containing Molecules: The Monobridged Isomer of Si_2H_2. *J. Chem. Phys.* **1992**, *97*, 7984–7989.
(17) Wang, X.; Andrews, L.; Kushto, G. P. Infrared Spectra of the Novel Ge_2H_2 and Ge_2H_4 Species and the Reactive $GeH_{1,2,3}$ Intermediates in Solid Neon, Deuterium and Argon. *J. Phys. Chem. A* **2002**, *106*, 5809–5816.

DOI: 10.1021/acs.jpclett.9b00284
J. Phys. Chem. Lett. 2019, 10, 1264–1271

(18) Yang, T.; Dangi, B. B.; Kaiser, R. I.; Chao, K. H.; Sun, B. J.; Chang, A. H. H.; Nguyen, T. L.; Stanton, J. F. Gas-Phase Formation of the Disilavinylidene (H_2SiSi) Transient. *Angew. Chem.* **2017**, *129*, 1284−1288.
(19) Grev, R. S.; Schaefer, H. F. The Remarkable Monobridged Structure of Si_2H_2. *J. Chem. Phys.* **1992**, *97*, 7990−7998.
(20) Jana, A.; Huch, V.; Scheschkewitz, D. NHC-Stabilized Silagermenylidene: A Heavier Analogue of Vinylidene. *Angew. Chem., Int. Ed.* **2013**, *52*, 12179−12182.
(21) Jana, A.; Majumdar, M.; Huch, V.; Zimmer, M.; Scheschkewitz, D. NHC-Coordinated Silagermenylidene Functionalized in Allylic Position and its Behaviour as a Ligand. *Dalton Transactions* **2014**, *43*, 5175−5181.
(22) Tomosada, A. E.; Kim, S.; Osamura, Y.; Yang, S. W.; Chang, A. H. H.; Kaiser, R. I. First Detection of the Silylgermylene (H_3SiGeH) and D4-Silylgermylene (D_3SiGeD) Molecules in Low Temperature Silane−Germane Ices. *Chem. Phys.* **2012**, *409*, 49−60.
(23) Levine, R. D. *Molecular Reaction Dynamics*; Cambridge University Press: Cambridge, U.K., 2005.
(24) Grice, R. Dynamics of Persistent Collision Complexes in Molecular Beam Reactive Scattering. *Int. Rev. Phys. Chem.* **1995**, *14*, 315−326.
(25) Lein, M.; Krapp, A.; Frenking, G. Why Do the Heavy-Atom Analogues of Acetylene E_2H_2 (E = Si−Pb) Exhibit Unusual Structures? *J. Am. Chem. Soc.* **2005**, *127*, 6290−6299.
(26) Chou, S.-L.; Lo, J.-I.; Peng, Y.-C.; Lin, M.-Y.; Lu, H.-C.; Cheng, B.-M.; Ogilvie, J. F. Identification of Diborane(4) with Bridging B-H-B Bonds. *Chemical Science* **2015**, *6*, 6872−6877.
(27) Kim, G.-S.; Nguyen, T. L.; Mebel, A. M.; Lin, S. H.; Nguyen, M. T. Ab Initio/RRKM Study of the Potential Energy Surface of Triplet Ethylene and Product Branching Ratios of the $C(^3P)$ + CH_4 Reaction. *J. Phys. Chem. A* **2003**, *107*, 1788−1796.
(28) Lu, I. C.; Chen, W.-K.; Huang, W.-J.; Lee, S.-H. Dynamics of the Reaction $C(^3P)$+SiH_4: Experiments and Calculations. *J. Chem. Phys.* **2008**, *129*, 164304.
(29) Kaiser, R. I.; Maksyutenko, P.; Ennis, C.; Zhang, F.; Gu, X.; Krishtal, S. P.; Mebel, A. M.; Kostko, O.; Ahmed, M. Untangling the Chemical Evolution of Titan's Atmosphere and Surface - From Homogeneous to Heterogeneous Chemistry. *Faraday Discuss.* **2010**, *147*, 429−478.
(30) Gu, X.; Guo, Y.; Kawamura, E.; Kaiser, R. I. Characteristics and Diagnostics of an Ultrahigh Vacuum Compatible Laser Ablation Source for Crossed Molecular Beam Experiments. *J. Vac. Sci. Technol., A* **2006**, *24*, 505−511.
(31) Vernon, M. F. *Molecular Beam Scattering*. Ph.D. Dissertation, University of California, Berkeley, CA, 1983.
(32) Weiss, P. S. *Reaction Dynamics of Electronically Excited Alkali Atoms with Simple Molecules*. Ph.D. Dissertation, University of California, Berkeley, CA, 1986.
(33) Sansonetti, J. E.; Martin, W. C. Handbook of Basic Atomic Spectroscopic Data. *J. Phys. Chem. Ref. Data* **2005**, *34*, 1559−2259.
(34) Purvis, G. D., III; Bartlett, R. J. A Full Coupled-Cluster Singles and Doubles Model: The Inclusion of Disconnected Triples. *J. Chem. Phys.* **1982**, *76*, 1910−1918.
(35) Hampel, C.; Peterson, K. A.; Werner, H.-J. A Comparison of the Efficiency and Accuracy of the Quadratic Configuration Interaction (QCISD), Coupled Cluster (CCSD), and Brueckner Coupled Cluster (BCCD) Methods. *Chem. Phys. Lett.* **1992**, *190*, 1−12.
(36) Knowles, P. J.; Hampel, C.; Werner, H.-J. Coupled Cluster Theory for High Spin, Open Shell Reference Wave Functions. *J. Chem. Phys.* **1993**, *99*, 5219−5227.
(37) Deegan, M. J.; Knowles, P. J. Perturbative Corrections to Account for Triple Excitations in Closed and Open Shell Coupled Cluster Theories. *Chem. Phys. Lett.* **1994**, *227*, 321−326.
(38) Peterson, K. A.; Woon, D. E.; Dunning, T. H., Jr Benchmark Calculations with Correlated Molecular Wave Functions. IV. The Classical Barrier Height of the H + H_2 → H_2 + H Reaction. *J. Chem. Phys.* **1994**, *100*, 7410−7415.
(39) Peterson, K. A.; Dunning, T. H., Jr Intrinsic Errors in Several *Ab Initio* Methods: The Dissociation Energy of N_2. *J. Phys. Chem.* **1995**, *99*, 3898−3901.
(40) Werner, H.-J.; Knowles, P.; Lindh, R.; Manby, F. R.; Schütz, M.; Celani, P.; Korona, T.; Rauhut, G.; Amos, R.; Bernhardsson, A. MOLPRO, version 2010.1, A Package of Ab Initio Programs; University of Cardiff: Cardiff, U.K., 2010; see http://www.molpro.net.
(41) Frisch, M. J.; Trucks, G. W.; Schlegel, H. B.; Scuseria, G. E.; Robb, M. A.; Cheeseman, J. R.; Scalmani, G.; Barone, V.; Mennucci, B.; Petersson, G. A. *Gaussian 09*, revision D. 01; Gaussian Inc.: Wallingford, CT, 2009.
(42) Nguyen, T. L.; McCaslin, L.; McCarthy, M. C.; Stanton, J. F. Communication: Thermal Unimolecular Decomposition of Syn-CH_3CHOO: A Kinetic Study. *J. Chem. Phys.* **2016**, *145*, 131102.
(43) Nguyen, T. L.; McCarthy, M. C.; Stanton, J. F. Relatively Selective Production of the Simplest Criegee Intermediate in a CH_4/O_2 Electric Discharge: Kinetic Analysis of a Plausible Mechanism. *J. Phys. Chem. A* **2015**, *119*, 7197−7204.
(44) Dunning, T. H. Gaussian-Basis Sets for Use in Correlated Molecular Calculations 0.1. The Atoms Boron through Neon and Hydrogen. *J. Chem. Phys.* **1989**, *90*, 1007−1023.
(45) Almlof, J.; Taylor, P. R. General Contraction of Gaussian-Basis Sets 0.1. Atomic Natural Orbitals for 1st-Row and 2nd-Row Atoms. *J. Chem. Phys.* **1987**, *86*, 4070−4077.
(46) Almlof, J.; Taylor, P. R. General Contraction of Gaussian-Basis Sets 0.2. Atomic Natural Orbitals and the Calculation of Atomic and Molecular-Properties. *J. Chem. Phys.* **1990**, *92*, 551−560.
(47) McCaslin, L. M.; Stanton, J. F. Calculation of Fundamental Frequencies for Small Polyatomic Molecules: A Comparison of Correlation-Consistent and Atomic Natural Orbital Basis Sets. *Mol. Phys.* **2013**, *111*, 1492−1496.
(48) Mills, I. M. Vibration−Rotation Structure in Asymmetric- and Symmetric-Top Molecules. In *Molecular Spectroscopy: Modern Research*; Rao, K. N., Mathews, C. W., Eds.; Academic Press: New York, 1972.
(49) Hoy, A. R.; Mills, I. M.; Strey, G. Anharmonic Force Constant Calculations. *Mol. Phys.* **1972**, *24*, 1265−1290.
(50) Stanton, J. F.; Gauss, J.; Harding, M. E.; Szalay, P. G.; Auer, A. A.; Bartlett, R. J.; Benedikt, U.; Berger, C.; Bernholdt, D. E.; Bomble, Y. J. *CFOUR, A Quantum Chemical Program Package*; 2009. For the current version, see http://www.cfour.de.

DOI: 10.1021/acs.jpclett.9b00284
J. Phys. Chem. Lett. 2019, 10, 1264−1271